

Quadrature Component Analysis for interferometry

J. Vargas*, C.O.S. Sorzano

Biocomputing Unit, Centro Nacional de Biotecnología-CSIC, C/Darwin 3, 28049 Cantoblanco Madrid, Spain

ARTICLE INFO

Article history:

Received 6 November 2012

Received in revised form

26 December 2012

Accepted 4 January 2013

Available online 29 January 2013

Keywords:

Phase demodulation

Interferometry

Principal Component Analysis

ABSTRACT

This work presents a generalization of the Principal Component Analysis (PCA) demodulation approach that is renamed as Quadrature Component Analysis. We show a new and general mathematical analysis of this demodulation algorithm and we demonstrate that this method is not affected by the number of fringes limitation. Additionally, we show that any asynchronous phase-shifting demodulation method is affected by a global phase sign indetermination, if no information is given about the phase-shifts. We have tested the proposed method with simulated and experimental interferograms obtaining satisfactory results. A complete MATLAB software package is provided in [<http://goo.gl/JWNUr>].

© 2013 Elsevier Ltd. All rights reserved.

1. Introduction

Interferometry is a powerful tool that is used in numerous industrial, research and development applications. These include measuring the quality of a variety of manufactured items such as hard disks, drives and magnetic recording heads, laser and optics for CD and DVD drives, cameras, laser printers, machined parts and components for fiber-optic systems among others. The primary reasons interferometry is so useful is because of its non-contact and non-destructive nature and because it provides very high accuracy and precision—within the nanometer or even angstrom range. Phase-Shifting Interferometry (PSI) is the most used interferometry technique in optical metrology for measuring the modulating phase of interferograms.

Recently, a new asynchronous phase-shifting demodulation method based on the Principal Component Analysis (PCA) algorithm, which can extract the phase distribution from unknown randomly phase-shifted interferograms, has been proposed [1,2]. This method has attracted the attention of the research community and different variants and applications have been proposed since its publication [3–7]. The PCA demodulation approach is very fast—approximately two orders of magnitude faster than the Advanced Iterative Algorithm (AIA) [8] as it is not iterative and it does not require performing a non-linear optimization. Additionally, the PCA method does not need the background illumination and contrast to be spatially constant. In [2–4] it is presented that the main drawback of this approach is that its application range is limited to modulating phases that varies

more than 2π (rad) in the observed area. Therefore, it needs more than one fringe in the resultant interferograms. We call this restriction as the number of fringes limitation, that is an important issue because interferograms that come from very flat modulating phases must not be processed using this approach. Therefore, this method cannot be used in non-contact quality control processes of high quality optical components. In order to solve this limitation, in [3,4] it has been proposed combining both the PCA and the least squares minimization method. Obviously, these two-step approaches require considerably more complexity and processing load than the original PCA algorithm and the fast processing velocity of the original PCA method is compromised. Moreover, in [3] the authors present an additional drawback of the PCA demodulation approach that consists in the limitation of this approach to determine the global sign of the absolute phase. They propose to solve this sign indetermination using the further asynchronous least squares minimization demodulation method.

In this work, we present a generalization of the Principal Component Analysis (PCA) demodulation approach, which is renamed as Quadrature Component Analysis (QCA), and we show that this approach is not affected by the number of fringes limitation. Additionally, here, we show that the indetermination in the global sign of the absolute phase is not a particular problem of the PCA demodulation method and it is common to any asynchronous approach, if no information is given about the phase-shifts. Therefore, it is not possible to determine the phase global sign with a non-linear optimization as it is claimed in [3].

In Section 2, we present the theoretical foundations and mathematical analysis of the Quadrature Component Analysis method. Section 3 includes some simulations and in Section 4, we show the experimental results. Finally, in Section 5, the conclusions are drawn.

* Corresponding author. Tel./fax: 34 91 5854506.

E-mail addresses: jvargas@fis.ucm.es, jvargas@cnb.csic.es (J. Vargas).

2. Theoretical foundations

In PSI, an interferogram sequence of N samples can be described using the following expression:

$$I_n = a + b \cos[\Phi + \delta_n] \quad n = [1, N] \quad (1)$$

where $a = a(x, y)$ is the background component, $b = b(x, y)$ is the modulation term, $\Phi = \Phi(x, y)$ is the phase map and δ_n are the phase-steps that are randomly distributed. Note that the spatial dependence has been omitted for the sake of clarity. Expression (1) can be rewritten as:

$$I_n = a + b(\cos[\Phi]\cos[\delta_n] - \sin[\delta_n]\sin[\Phi]) \quad (2)$$

From Eq. (2) and grouping terms, we obtain:

$$I_n = a + \alpha_{1n}I_c + \alpha_{2n}I_s \quad (3)$$

where $\alpha_{1n} = \cos[\delta_n]$, $\alpha_{2n} = -\sin[\delta_n]$ and $I_c = b \cos[\Phi]$, $I_s = b \sin[\Phi]$ correspond to the quadrature signals. From a set of interferograms the background can be estimated by a temporal average as:

$$a \cong \sum_{n=1}^N I_n / N \quad (4)$$

and Eq. (3) can be rewritten as:

$$\tilde{I}_n = I_n - a = \alpha_{1n}I_c + \alpha_{2n}I_s \quad (5)$$

From Eq. (5), we see that a background filtered interferogram can be expressed as a linear combination of two signals. Therefore, a phase-shifted interferogram sequence belongs to a two-dimensional vector subspace. Expression (5) can be rewritten as:

$$\tilde{I} = Q A \quad (6)$$

with

$$A = [\alpha_1, \alpha_2]^T \quad (7)$$

where A is a $2 \times N$ matrix, α_1 and α_2 are column vectors of size $N \times 1$ and $[\cdot]^T$ denotes the transposing operation. Q is a matrix of size $N_x N_y \times 2$. This matrix is formed by the quadrature components as:

$$Q = [q_1, q_2] \quad (8)$$

where q_1 and q_2 are column vectors with size $N_x \times N_y$, whose elements are taken columnwise from I_c and I_s respectively. Finally, \tilde{I} is a matrix with size $N_x N_y \times N$ where the n th column is taken columnwise from \tilde{I}_n . Observe that $A A^T$ corresponds to:

$$A A^T = \begin{pmatrix} \|\alpha_1\|^2 & \langle \alpha_1, \alpha_2 \rangle \\ \langle \alpha_1, \alpha_2 \rangle & \|\alpha_2\|^2 \end{pmatrix} \quad (9)$$

with $\|\cdot\|$ and $\langle \cdot, \cdot \rangle$ the norm and inner product operators. If the phase-shifts are approximately uniformly distributed in the $[0, 2\pi]$ range, we have that:

$$A A^T = \eta \begin{pmatrix} 1 & 0 \\ 0 & 1 \end{pmatrix} \quad (10)$$

with $\eta = \|\alpha_1\|^2 \cong \|\alpha_2\|^2$ and we can rewrite Eq. (6) as:

$$\tilde{I} = \hat{Q} \hat{\Lambda} \quad (11)$$

where $\hat{Q} = \sqrt{\eta} Q$ and $\hat{\Lambda} = \hat{\Lambda} / \sqrt{\eta}$. The covariance matrix C of \tilde{I} is given by:

$$C = \tilde{I}^T \tilde{I} = \hat{\Lambda}^T \hat{M} \hat{\Lambda} \quad (12)$$

where, $\hat{M} = \hat{Q}^T \hat{Q}$ and it is given by:

$$\hat{M} = \begin{pmatrix} \|\hat{q}_1\|^2 & \langle \hat{q}_1, \hat{q}_2 \rangle \\ \langle \hat{q}_1, \hat{q}_2 \rangle & \|\hat{q}_2\|^2 \end{pmatrix} \quad (13)$$

Because \hat{M} is real and symmetric, it is possible diagonalizing it and Eq. (12) can be rewritten as:

$$\tilde{I}^T \tilde{I} = \hat{\Lambda}^T (\hat{U}^T \hat{D}_Q \hat{U}) \hat{\Lambda} \quad (14)$$

where, \hat{U} and \hat{D}_Q are orthogonal and diagonal matrixes both with size 2×2 . We can define $\hat{A} = \hat{U} \hat{\Lambda}$ and rewrite Eq. (14) as:

$$\tilde{I}^T \tilde{I} = \hat{A}^T \hat{D}_Q \hat{A} \quad (15)$$

If $\eta = \|\alpha_1\|^2 \cong \|\alpha_2\|^2$ and $\hat{\Lambda}$ is an orthogonal matrix, \hat{A} is also an orthogonal matrix as the set of orthogonal matrixes form a group. Strictly $\hat{\Lambda}$ is not orthogonal as it is not square but we can generate an orthogonal matrix from the two orthonormal rows of $\hat{\Lambda}$ by the cross product. Observe that if this approximation is fulfilled, we can rewrite \tilde{I} as:

$$\tilde{I} = \hat{Q} (\hat{U}^T \hat{A}) = (\hat{Q} \hat{U}^T) \hat{A} = \hat{Y} \hat{A} \quad (16)$$

PCA is a technique from statistics for reducing an image or dataset that transforms a number of possibly correlated images into the smallest number of uncorrelated images called the principal components. The interferogram dataset shown in Eq. (6) can be expressed as:

$$\tilde{I} = [i_1, i_2, \dots, i_N] \quad (17)$$

where i_n is a column vector with size $N_x N_y$, whose elements are taken columnwise from the n th image \tilde{I}_n . The covariance matrix, $C = \tilde{I}^T \tilde{I}$ is real and symmetric and then always is possible to diagonalize this matrix as:

$$C = A^T D A \quad (18)$$

where A and D are orthogonal and diagonal matrixes respectively, both with size $N \times N$. Observe that this factorization is unique if all the eigenvalues are distinct. If there are two equal eigenvalues, then the factorization is unique up to interchanges in the respective columns of A . The orthogonal matrix A rotates the original vector set \tilde{I} to a new basis in which the different vectors are orthogonal between them and are given as:

$$Y = \tilde{I} A^T \quad (19)$$

$$\tilde{I} = Y A$$

where Y is a matrix of size $N_x N_y \times N$ and its column vectors y_n are orthogonal and uncorrelated. They correspond to the principal components of the interferogram set that belongs to a two-dimensional vector subspace, we are only concerned about the two first principal components with the largest eigenvalues denoted as y_1 and y_2 [1,2]. Taking into account that the matrix factorization shown in (15) and (16) is unique; we can asseverate that the first and second principal components of Y corresponds to \hat{Y} and that the orthogonal matrix A to \hat{A} . Note that this is valid, if the phase-shifts are approximately uniformly distributed in the $[0, 2\pi]$ range. Observe that the principal components (y_1, y_2) relate to the true quadrature components (q_1, q_2) by,

$$y_i = \hat{y}_i = \hat{q}_i \hat{U}^T, \quad i = 1, 2 \quad (20)$$

where, \hat{U}^T is an unknown orthogonal matrix if we have not information about the phase-shifts. Note that the only effect of \hat{U}^T is an unknown phase-shift or piston term in the obtained modulating phase, that is obtained by,

$$\Phi = \arctan(I_s/I_c) = \pm \arctan(y_2/y_1) \quad (21)$$

Observe that there is an indetermination in the global phase sign because we arbitrarily assign the cosine and sine signals to the first and second principal components. This indetermination is common to any asynchronous phase-shifting approach, if no additional information is given about the phase-shifts. Observe that we can generate an identical interferogram set, than the one

presented in Eq. (2) if we change Φ by $-\Phi$ and δ_n by $-\delta_n$ and there is no way to know the sign of the modulating phase, if no information about the phase-steps is given. Note that we can easily determine the phase sign imposing experimentally that the first and second phase-shift has to be in the first quadrant that it is not very demanding. Observe that in this case, the first and second interferograms have the following mathematical expression, which is from Eq. (2):

$$\begin{aligned} I_1 &= a + b \cos[\Phi] \\ I_2 &= a + b(\cos[\Phi]\cos[\delta_2] - \sin[\delta_2]\sin[\Phi]) \end{aligned} \quad (22)$$

where we have used without loss of generality that $\delta_1=0$. As δ_2 is in same quadrant, than δ_1 (first quadrant), we know that both $\cos[\delta_2]$ and $\sin[\delta_2]$ are positive valued. Therefore, in this case there is no sign ambiguity and we can use a two-step phase-shifting demodulation approach [10–12] to obtain a coarse modulating phase that is not affected by the sign ambiguity problem. Finally, we can use this coarse modulating phase to correct the sign of our determined phase by the QCA method, that uses all the interferograms.

3. Simulations

In order to verify our mathematical analysis, we have performed some simulations. We will use QCA and AIA to refer to the Quadrature Component Analysis and to the Advanced Iterative Algorithm [8]. We use an interferogram set composed by 20 fringe patterns. The interferograms have a size of 640×480 pixels. The modulating phase, background and modulation signals are Gaussian shaped and their mathematical expressions corresponds to:

$$\begin{aligned} a(x,y) &= 0.5 + 0.3 \exp(-5((x-10)^2 + (y-15)^2)/1e5) \\ b(x,y) &= \exp(-(x^2 + y^2)/1e5) \\ \Phi(x,y) &= \pi \exp(-(x^2 + y^2)/1e5) \end{aligned} \quad (23)$$

where (x,y) correspond to pixel coordinates and the origin of coordinates is placed in the image center. The noise is additive with a standard normal distribution, and the signal to noise ratio

is 10%. In Fig. 1, we show the first four interferograms of the sequence. As can be seen from Fig. 1, there is less than one fringe in the interferograms. In Fig. 2, we show a profile along column 240 pixels of the retrieved phases by the QCA, and AIA methods. Additionally we show the profile of the reference phase. As can be seen from Fig. 2, the QCA and AIA phases are similar to the reference phase. The retrieved root-mean-square error (rms) of the difference between the reference and the retrieved phases, and the processing times are 0.076 rad and 0.16 for the rms errors and 0.60 s and 46 s for the processing times when we use the QCA and AIA respectively. Note that the QCA is the fastest and most accurate method in this case. In the second experiment, we analyze the accuracy of the retrieved phase with respect to the number of fringes in the interferograms. We use the same interferogram set than in the case before, but we change the dynamic range of the modulating phase for each interferogram set. In Fig. 3, we show the resultant first interferogram for each interferogram set. As can be seen from Fig. 3, the first interferograms are composed by modulating phases with low dynamic ranges and have less than one fringe. The last interferograms have more than two fringes. In Fig. 4(a) and (b), we show the obtained rms of the difference between the reference and the retrieved

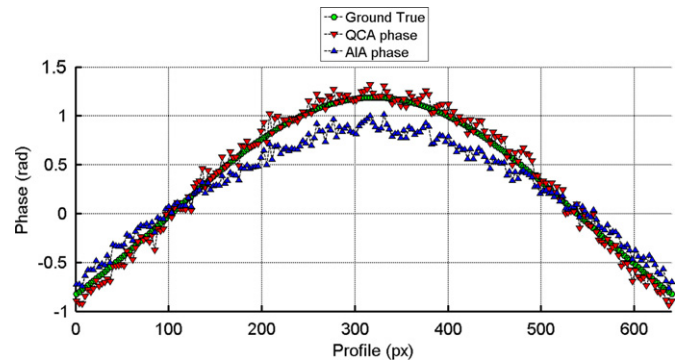


Fig. 2. Profile along row 240 pixels of the retrieved phases by the QCA, and AIA methods obtained in the first simulation.

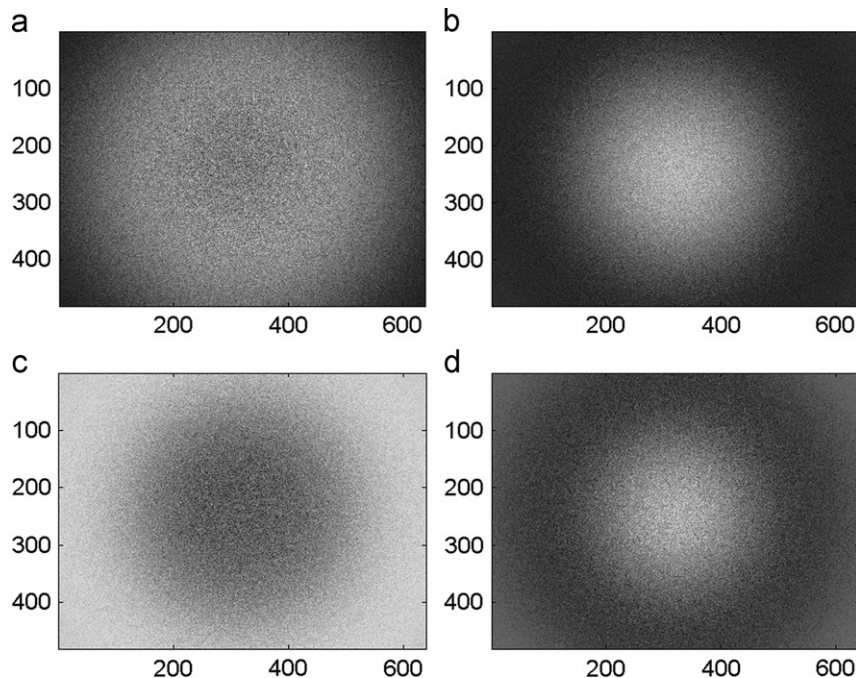


Fig. 1. First four interferograms used in the first simulation.

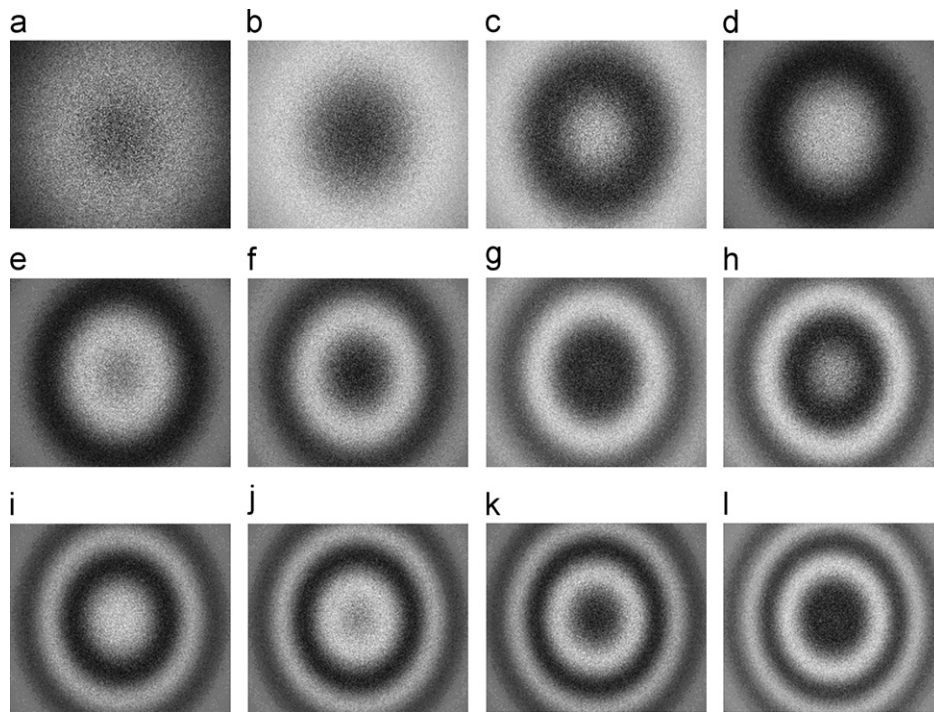


Fig. 3. Interferograms from 12 modulating phases with different dynamic ranges.

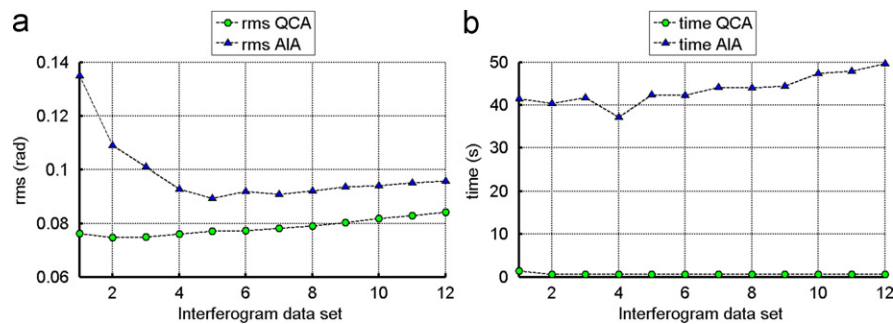


Fig. 4. Root-mean-square errors (rms) (a) and processing times (b) obtained when processing with the QCA and AIA methods.

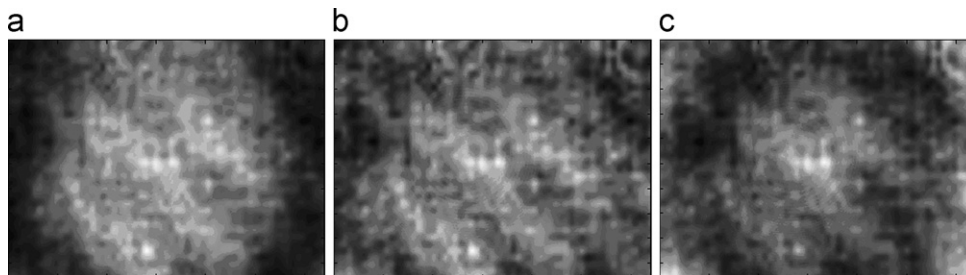


Fig. 5. First three experimental interferograms.

phases and the processing times obtained when processing with the QCA and AIA methods. As can be seen from Fig. 4, the QCA is not affected by the dynamic range of the modulating phase and therefore by the number of fringes limitation. Additionally, the QCA is the method that presents the best accuracy.

4. Experimental results

We have also tested the different methods with experimental interferograms. We have obtained five interferograms with

equidistant phase-shifts with values $[0, \pi/2, \pi, 3\pi/2, 2\pi]$ (rad) using a Mach–Zehnder interferometer and measuring a glass plate. The interferograms have a size of 640×480 pixels. The first three interferograms are shown in Fig. 5. Observe from Fig. 5, that there is less than one fringe in the interferograms. We have used the synchronous Schwider–Hariharan 5-step algorithm [9] to obtain a reference phase. Additionally, with the same interferograms we have obtained the modulating phase using the QCA and AIA methods. The computed phases are shown in Fig. 6. The rms of the difference between the reference, and the retrieved phases and the processing times are 0.052 rad

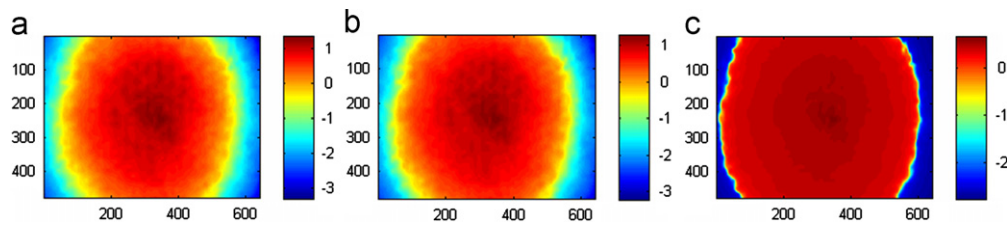


Fig. 6. Reference phase map (a), and phases by the proposed QCA (b), and AIA (c) methods obtained using real interferograms.

and 0.57 and 0.15 s and 45 s when we use the QCA and AIA respectively

5. Conclusions

In this work, we have presented a generalization of the Principal Component Analysis (PCA) demodulation approach, that it has been renamed as Quadrature Component Analysis. We have demonstrated analytically that this method is not limited by the number of fringes presented in the interferograms and, therefore, can be used to demodulate interferograms that come from very flat modulating phases. We have showed that the indetermination in the global phase sign is a limitation of any asynchronous demodulation method if no additional information is given about the phase-shifts. We have tested the proposed method with simulated and experimental interferograms obtaining satisfactory results. A complete MATLAB software package is provided in [<http://goo.gl/JWNUr>].

References

- [1] Vargas J, Antonio Quiroga J, Belenguer T. Phase-shifting interferometry based on principal component analysis. *Opt Lett* 2011;36(8):1326–8.
- [2] Vargas J, Antonio Quiroga J, Belenguer T. Analysis of the principal component algorithm in phase-shifting interferometry. *Opt Lett* 2011;36(12):2215–7.
- [3] Xu J, Jin W, Chai L, Xu Q. Phase extraction from randomly phase-shifted interferograms by combining principal component analysis and least squares method. *Opt Express* 2011;19(21):20483–92.
- [4] Vargas J, Sorzano COS, Estrada JC, Carazo JM. Generalization of the principal component analysis method for interferometry. *Opt Commun* 2012;286:130–4.
- [5] Xu J, Jin W, Chai L, Xu Q. Principal component analysis of multiple-beam Fizeau interferograms. *Opt Express* 2011;19(15):14464–72.
- [6] Du Y, Feng G, Li H, Vargas J, Zhou S. Spatial carrier phase-shifting algorithm based on principal component analysis method. *Opt Express* 2012;20(15):16471–9.
- [7] Du H, Zhao H, Li B, Cao S. Three frames phase-shifting shadow moiré using arbitrary unknown phase steps. *Meas Sci Technol* 2012;23(10):105201–7.
- [8] Wang ZY, Han BT. Advanced iterative algorithm for phase extraction of randomly phase-shifted interferograms. *Opt Lett* 2004;29(14):1671–3.
- [9] Hariharan P, Oreb BF, Eiju T. Digital phase-shifting interferometry: a simple error compensating phase calculation algorithm. *Appl Opt* 1987;26(13):2504–6.
- [10] Vargas J, Quiroga JA, Belenguer T, Servín M, Estrada JC. Two-step self-tuning phase-shifting interferometry. *Opt Express* 2011;19(2):638–48.
- [11] Vargas J, Quiroga JA, Sorzano COS, Estrada JC, Carazo JM. Two-step interferometry by a regularized optical flow algorithm. *Opt Lett* 2012;36(17):3485–7.
- [12] Vargas J, Quiroga JA, Sorzano COS, Estrada JC, Carazo JM. Two-step demodulation based on Gram-Schmidt orthonormalization method. *Opt Lett* 2012;37(3):443–5.